Microfiber Bragg Grating with Zinc Oxide Nanorod Arrays for Temperature Sensing

Aisyah M. Aris, Husna A. Rahman and Sulaiman W. Harun

Abstract—**Previous works utilizing fiber Bragg grating (FBG) for sensing temperature differences often reported on complexity of the design due to the multi-parameter sensor configuration. Sole FBG based temperature sensor on the other hand commonly suffers from limited measurement range and low sensitivity. In this paper, a zinc oxide (ZnO) nanorods integrated silica microfiber Bragg grating sensor is developed for the measurement of temperature ranging from 50°C to 150°C. The spectral responses of the proposed sensor are monitored using optical spectrum analyzer (OSA) to observe its Bragg wavelength shift and are compared with those from bare FBG. When subjected to increasing ambient temperature, the hydrothermally synthesized ZnO nanorod arrays experienced higher thermal expansion and thus, exhibited better performance than its bare counterpart with measured temperature sensitivity of 13.6 pm/°C and 10.9 pm/°C, respectively. The sensor resolution also significantly improved due to the growth of ZnO nanorod arrays on the taper surface by reducing the original resolution from 0.48°C to 0.02°C.**

Index Terms—**fiber Bragg grating (FBG), microfiber, zinc oxide nanorods, temperature sensor**

I. INTRODUCTION

FIBER Bragg grating (FBG) has become a favorable option as an intrinsic fiber optic sensor widely used for various sensor applications [1-3]. Due to its electrically passive operation, immunity to electromagnetic interference (EMI), lightweight, small size, high sensitivity and multiplexing capabilities [4], this type of in-fiber grating [5] is highly suitable for implementation at rugged area that poses difficult measurement challenges. FBG is formed from periodic modulation in the refractive index of the core of an optical fiber. A narrow wavelength of a broadband pulse that propagates down the fiber is reflected by successive grating planes while the rest of the pulse is transmitted [6]. The narrow wavelength is known as Bragg wavelength, λ_B and is dependent on the FBG parameters represented as in (1)

$$\lambda_B = 2n_{eff} \Lambda_B \tag{1}$$

where, n_{eff} is the effective refractive index of the fiber core and Λ_B is the spacing between gratings, known as the grating period. As variations in strain and temperature are known to affect n_{eff} and Λ_B, and consequently alter the Bragg wavelength, this principle is ideal for applying FBG as a temperature sensor.

Numerous studies have reported works on FBG and its temperature characteristics. Recent works published so far mostly involved simultaneous measurement of temperature and other parameters such as strain [7], liquid level [8], displacement [9] and refractive index [10]. Though FBGs are suitable for multiple real-time monitoring, further work is often required to discriminate between the dual-parameter measurements. Li et al. [11] reported on a simultaneous liquid level and temperature sensor based on an asymmetrical fiber Mach–Zehnder interferometer combined with a fiber Bragg grating. The sensor offers low cost fabrication but at the expense of a low temperature sensitivity of 10 pm/°C. Hu et al. [12] on the other hand published work on a fiber optic surface plasmon resonance (SPR) sensor for refractive index and temperature measurement based on a multimode fiber (MMF)-FBG-MMF structure. The complex sensor structure in addition to the silver film coating nevertheless guaranteed a maximum sensitivity of about 172pm/°C, though with a limited measurement range of 30°C to 65°C.

In the case of a single functional temperature sensor, Yucel et al. [13] presented a simulation design on an FBG multiple temperature sensor by multiplexing five FBGs using wavelength division multiplexing (WDM) technique to measure a temperature range of 0°C to 60°C with an achieved sensitivity of 10 pm/°C. A novel patent pending ultra high resolution optical fibre temperature sensor has also been reported by Poeggel et al. [14]. The ultra high temperature sensitivity of 8.77 nm/K is the highest reported value so far but comes with a high degree of complexity in terms of its fabrication. Furthermore, the extremely sensitive sensor is only able to detect a small temperature variations of 7K, which makes it unsuitable for commercial use. Thus, work by Hsiao et al. [15] offers a good alternative to previous reports in which an FBG is coated with a metal coating i.e. chromium nitride (CrN) to enhance the sensor's sensitivity. The metal-coated sensor exhibited a 15.5 pm/°C greater temperature sensitivity than the bare FBG when detecting temperature in the range of 450°C until 650°C. However, the sensitivity decreased to 13 pm/°C for measurement below 450°C, making

it more fitted for high temperature sensing.

In this research, we proposed a simple and inexpensive approach for the fabrication of a temperature sensor using microfiber Bragg grating with ZnO nanorod arrays hydrothermally synthesized on its tapered surface. For a metal-coated FBG sensor, the layer of coating is known to expand and contract during temperature fluctuations. Thus, this work is aimed at studying the effects of ZnO nanorods coating in improving the performance of the FBG temperature sensor.

II. METHODOLOGY

A uniform fiber Bragg grating written in a commercially available hydrogenated B/Ge co-doped photosensitive single mode fiber (Fibercore Ltd.: PS1250/1500) with a core and a cladding diameter of 9 µm and 125 µm, respectively is used in this research as a medium to grow the ZnO nanorods. The length of the inscribed gratings is 2 cm whereas the Bragg wavelength is at 1559 nm.

A. Microfiber Fabrication

Fabrication of microfiber is essential prior to the synthesis of ZnO nanorods on its surface. Chemical etching method is used to taper the grating part through immersion in a hydrofluoric acid (HF) solution of 46% concentration at room temperature inside a fume chamber. The continuous thinning of the cladding region as a result of the reaction between HF and silica glass eventually produced a fiber taper with a diameter of 10 µm following a 165 minutes etching time. Fig. 1 illustrates the chemical etching process performed in order to taper the fiber at its Bragg grating location.
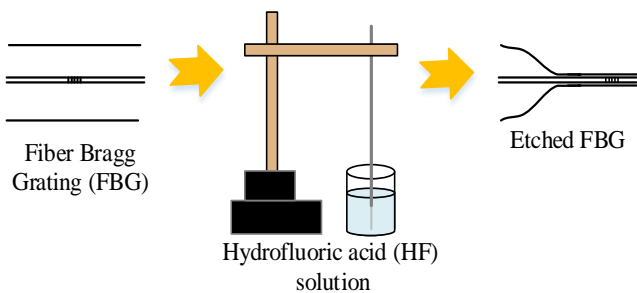

Fig. 1.Chemical etching process of an FBG

B. Synthesis of Zinc Oxide Nanorods

The ZnO nanorods are synthesized on the tapered surface through hydrothermal technique in [16] which involved two major procedures, i.e. seeding and growth.

1) Seeding:

The seeding solution is made from two precursor solutions of 1 mM in concentration each, namely A and B. Solution A is prepared by dissolving 0.0008 g of sodium hydroxide (NaOH) [Merck] in 20 ml of ethanol (C_2H_6O) [95%, HmbG]. The mixture is heated slowly for 15 minutes on a hot plate at 50°C under continuous stirring. Solution B on the other hand is composed of 0.00439 g of zinc acetate dihydrate

($Zn(CH_3COO)_2 \cdot 2H_2O$) [Grade AR, Friendemann Schmidt] and 20 ml of ethanol (C_2H_6O) [95%, HmbG] stirred together at 50°C for a period of 30 minutes. The solution is left to cool down for a few minutes before another 20 ml of ethanol is added to it. Next, solution A is dropped gradually into solution B under constant stirring in order to combine both precursor solutions. Finally, it is placed in a water bath at 60°C for 3 hours.

Using the prepared seeding solution, a seed layer is deposited on the taper surface through slow stirring method. This seed layer serves as the nucleation site for the growth of ZnO nanorods. In this method, the taper of the microfiber is suspended in the seeding solution and undergo continuous slow stirring process at 150 rpm for 30 minutes without any heat applied. The microfiber is then left to anneal for 3 hours at a temperature of 90°C. Fig. 2 shows the seeding process of the ZnO nanorods synthesis.
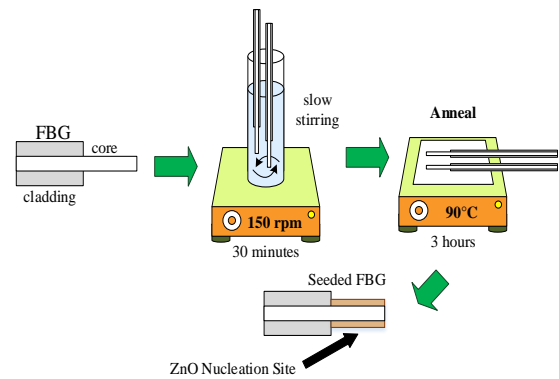

Fig. 2.Seeding process of ZnO nanorods synthesis

2) Growth

The growth process is carried out subsequent to the end of the annealing time. In this process, the seeded FBG is placed vertically inside a beaker filled with 10 mM growth solution that consists of 0.280372 g of hexamethylenetetramine ($C_6H_{12}N_4$) [99%, Sigma-Aldrich] and 0.59498 g of zinc nitrate hexahydrate ($Zn(NO_3)_2 \cdot 6H_2O$) [98%, Sigma-Aldrich] dissolved in 200 ml of deionized (DI) water. It is then inserted into a vacuum oven set to a temperature of 90°C to undergo 8 hours of growth time. Fig. 3 depicts the steps taken during the growth process. Once the growth time ended, the coated fiber is taken out from the solution to be rinsed with DI water and left to dry at normal room conditions.
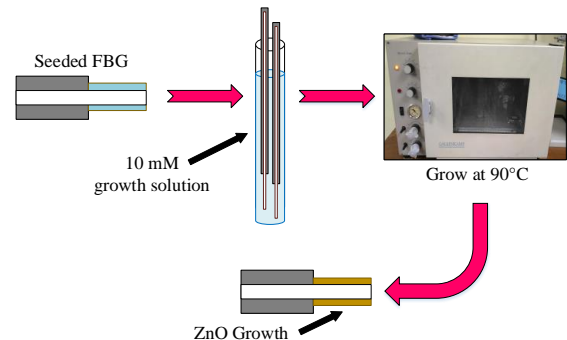

Fig. 3.Growth process of ZnO nanorods synthesis

C. Surface Morphology

The morphology of ZnO nanorod and its chemical composition are investigated using a field emission scanning electron microscope (FESEM) equipped with an energy-dispersive x-ray spectroscopy (EDS) operated at 5 kV. Fig. 4 displays the FESEM image of ZnO nanorods grown on the taper surface of an FBG at 30,000x magnification. The image shows a compact and monodispersed growth of nanorod arrays on the surface. Inset of Fig. 4 corresponds to higher magnification image of the nanorods which reveals that the ZnO nanorods possess hexagonal wurtzite crystal structure with an average diameter of 39 nm. Referring to prior work by Bora et al. [17] using the same hydrothermal technique but synthesized on a silica MMF, the average length of a nanorod from 8 hours of growth time was estimated to be 2 µm. This large surface-to-volume ratio characteristic of the ZnO nanorods enables better interaction with surrounding temperature changes and produces significant result despite the small temperature variations.

For the purpose of verifying the elemental composition of the nanorods, an EDS analysis is done on a sample of the fiber. Fig. 5 represents the result obtained from the analysis on the inspection area (inset Fig. 5) that indicates the synthesized nanorods are truly made of pure zinc (Zn) and oxygen (O) with weight percentage of 72.62% and 24.76%, respectively.
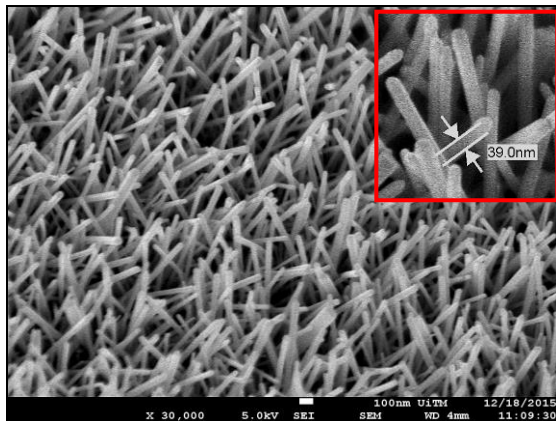

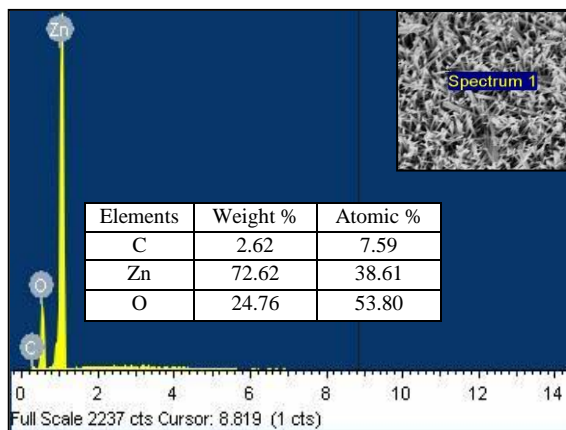Fig. 4.FESEM image of ZnO nanorod arrays grown on the taper surface

Elements	Weight %	Atomic %
C	2.62	7.59
Zn	72.62	38.61
O	24.76	53.80

Fig. 5.EDS analysis on ZnO nanorods grown on the taper surface

D. Experimental Setup

Reflection mode is employed for the measurement of temperature changes as configured in Fig. 6, in which an amplified spontaneous emission (ASE) from an erbium doped fiber amplifier (EDFA) is connected to an optical spectrum analyzer (OSA) [Anritsu MS9710C] set to a resolution of 0.05 nm. One end of the fiber is linked to the ASE source whereas the other end (taper) is directly placed on a hot plate surface [Corning PC-420D] with increasing temperature. A thermocouple rod attached to a multimeter [Pro'sKit MT-1860] is fixed close to the fiber to measure the actual temperature sensed by the fiber probe during the experiment. The multimeter is able to detect a temperature difference of 0.1°C.

In the experiment, the tapered FBG is tested under normal room conditions for a temperature range of 50°C to 150°C with a step increment of 10°C. In order to measure the performance of ZnO nanorods coating on the taper surface, the coated tapered FBG is tested against its bare counterpart. Data on reflection spectra attained at each desired temperature level are recorded to determine the wavelength shift due to the temperature differences sensed by the fiber probe.
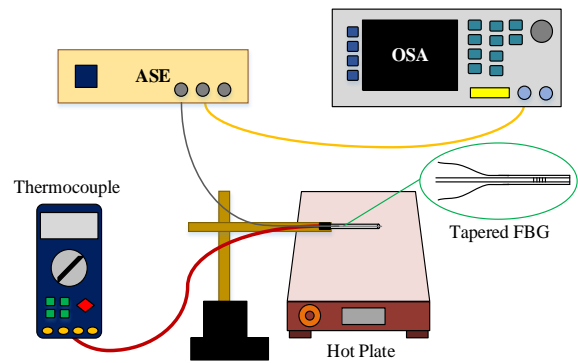

Fig. 6.Measurement setup for temperature sensing

III. RESULTS AND DISCUSSION

The temperature responsivity of each FBG sensor is investigated as light is injected into the core by the broadband laser from the ASE source. Fig. 7 presents the temperature dependence spectral response of bare and ZnO coated microfiber Bragg grating as a function of increasing temperature. As the temperature rises, both sensors experienced increments in the Bragg wavelength value resulted from changes in the effective refractive index and the grating period. The amount of wavelength shift at different temperatures for both bare and ZnO nanorods coating are compared. The experimental results show that the ZnO nanorods coating displays dominant temperature sensitivity and linearity of 13.6 pm/°C and 99.37%, respectively in comparison to the bare FBG with a temperature sensitivity value of 10.9 pm/°C and a linear fit of 98.98%.

The Bragg wavelength shift, $\Delta\lambda_B$ induced by the temperature variation can be expressed as in (2)

$$\Delta\lambda_B = \lambda_B[\alpha_{th} + \xi]\Delta T \qquad (2)$$

Where α indicates the thermal expansion coefficient of glass fiber, ξ denotes the fiber thermo-optic coefficient and ΔT is the changes in temperature [18, 19]. According to Hsiao et al. [15], for metal-coated FBG, changes in temperature causes perturbation to the grating period as a result of thermal expansion of the fiber as well as strain generated from thermal expansion of the metal coating. Moreover, the refractive index (RI) of the core is also modified due to the thermo-optic effect. In a study reported by Lee et al. in [20], exposure to increasing temperature causes ZnO nanowire to expand due to pyroelectric properties of ZnO. Since ZnO has higher thermal expansion coefficient of 4.75×10^{-6} K^{-1} [21] than silica which is 0.55×10^{-6} K^{-1}, this explains the bigger wavelength shift observed after coating the microfiber with ZnO nanorod arrays. Additionally, as the refractive index of ZnO is known to be 2.00 which is much higher than RI of silica, this factor also resulted in a larger effective refractive index, and correspondingly triggered a greater amount of Bragg wavelength shift seen from the graph.

Table I compares the performance of the bare and ZnO nanorods coating utilized in the temperature sensing experiment. As previously mentioned, the sensitivity of the sensor has been enhanced by the growth of ZnO nanorod arrays on the fiber surface, indicated by almost 25% improvement from the bare fiber. Furthermore, the ZnO coated sensor also exhibited a much smaller standard deviation value of 0.28 pm against 5.2 pm observed from the uncoated sensor. The huge difference in these values significantly reduced the sensor resolution of the bare FBG from 0.48°C to 0.02°C, a 24 times enhancement achieved through the synthesis of ZnO nanorods coating on a normal tapered FBG.
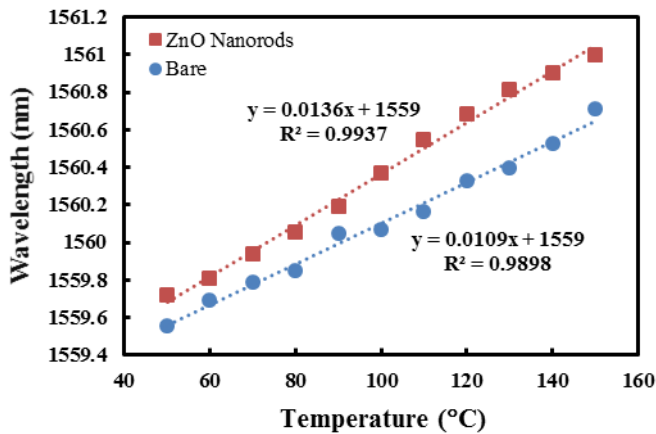
TABLE I
PERFORMANCE OF TEMPERATURE SENSOR

Parameter	Bare	ZnO Nanorods
Sensitivity (pm/°C)	10.9	13.6
Linearity (%)	98.98	99.37
Linear Range (°C)	50 - 150	50 - 150
Standard Deviation (pm)	5.2	0.28
Resolution (°C)	0.48	0.02

Hysteresis computation is essential to evaluate the stability of the proposed temperature sensor with embedded ZnO nanorod arrays. Hence, spectral responses from two different runs i.e. increasing and decreasing value of temperature gradient between 50°C to 150°C are recorded and compared. As shown in Fig. 8, the decreasing temperature plot only showcased a slight deviations from the increasing temperature plot with the maximum difference of 0.0943 nm, observed at the temperature of 130°C. Thus, the hysteresis percentage is calculated to be 7.26%, an acceptable value from a full scale output of 1.2992 nm.
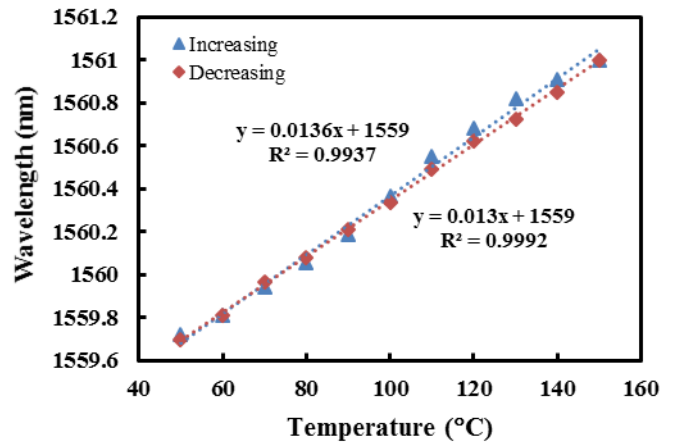

Fig. 8.Hysteresis plot obtained for temperature sensor employing ZnO nanorods coated micro-FBG

IV. CONCLUSION

A novel microfiber Bragg grating sensor with ZnO nanorod arrays grown on the taper surface has been demonstrated for the measurement of temperature within the range of 50°C to 150°C. The performance of the proposed sensor greatly improved in the presence of ZnO coating as shown by the 25% increase in its temperature sensitivity and 24 times reduction in its resolution over its bare counterpart. This proves that the ZnO nanorods coating is able to enhance the sensor's overall performance and offers good potential to be integrated in other sensor applications thanks to its low cost and simple fabrication that does not require complex vacuum environment.

Fig. 7.Temperature characterization of bare and ZnO coated microfiber Bragg grating

REFERENCES

[1] S. F. Correia, P. Antunes, E. Pecoraro, P. P. Lima, H. Varum, L. D. Carlos, *et al.*, "Optical fiber relative humidity sensor based on a FBG with a Di-ureasil coating," *Sensors,* vol. 12, pp. 8847-8860, 2012.

[2] R. M. Silva, G. Chesini, C. Gouveia, A. L. Ribeiro, O. Frazão, C. Cordeiro, *et al.*, "Magnetic field sensor with Terfenol-D thin-film coated FBG," in *OFS2012 22nd International Conference on Optical Fiber Sensor*, 2012, pp. 84213C-84213C-4.

[3] A. Wada, S. Tanaka, and N. Takahashi, "Optical fiber vibration sensor using FBG Fabry–Perot interferometer with wavelength scanning and Fourier analysis," *Sensors Journal, IEEE,* vol. 12, pp. 225-229, 2012.

[4] N. Sabri, S. Aljunid, M. Salim, and S. Fouad, "Fiber Optic Sensors: Short Review and Applications," in *Recent Trends in Physics of Material Science and Technology*, ed: Springer, 2015, pp. 299-311.

[5] T. Yeo, T. Sun, and K. Grattan, "Fibre-optic sensor technologies for humidity and moisture measurement," *Sensors and Actuators A: Physical,* vol. 144, pp. 280-295, 2008.

[6] A. Othonos, K. Kalli, D. Pureur, and A. Mugnier, "Fibre bragg gratings," in *Wavelength Filters in Fibre Optics*, ed: Springer, 2006, pp. 189-269.

[7] D. Ganziy, B. Rose, and O. Bang, "Performance of low-cost few-mode fiber Bragg grating sensor systems: polarization sensitivity and linearity of temperature and strain response," *Applied Optics,* vol. 55, pp. 6156-6161, 2016.

[8] O. F. Ameen, M. H. Younus, M. Aziz, A. I. Azmi, R. R. Ibrahim, and S. Ghoshal, "Graphene diaphragm integrated FBG sensors for simultaneous measurement of water level and temperature," *Sensors and Actuators A: Physical,* vol. 252, pp. 225-232, 2016.

[9] Y. Yu, H. Tam, W. Chung, and M. S. Demokan, "Fiber Bragg grating sensor for simultaneous measurement of displacement and temperature," *Optics letters,* vol. 25, pp. 1141-1143, 2000.

[10] T. DEY, P. Biswas, S. Bandyopadhyay, S. K. Bishnu, N. Basumallick, and S. Bandyopadhyay, "Reflection Type Superstructure Fiber Bragg Grating for Simultaneous Measurement of Refractive Index and Temperature," in *International Conference on Fibre Optics and Photonics*, 2016, p. Th3A. 64.

[11] C. Li, T. Ning, C. Zhang, X. Wen, J. Li, and C. Zhang, "Liquid level and temperature sensor based on an asymmetrical fiber Mach–Zehnder interferometer combined with a fiber Bragg grating," *Optics Communications,* vol. 372, pp. 196-200, 2016.

[12] T. Hu, Y. Zhao, and A.-n. Song, "Fiber optic SPR sensor for refractive index and temperature measurement based on MMF-FBG-MMF structure," *Sensors and Actuators B: Chemical,* vol. 237, pp. 521-525, 2016.

[13] M. Yucel, N. F. Ozturk, and C. Gemci, "Design of a Fiber Bragg Grating multiple temperature sensor," in *Digital Information and Communication Technology and its Applications (DICTAP), 2016 Sixth International Conference on*, 2016, pp. 6-11.

[14] S. Poeggel, D. Duraibabu, G. Dooly, E. Lewis, and G. Leen, "Novel ultrahigh resolution optical fibre temperature sensor," in *Sixth European Workshop on Optical Fibre Sensors (EWOFS'2016)*, 2016, pp. 991605-991605-4.

[15] T.-C. Hsiao, T.-S. Hsieh, Y.-C. Chen, S.-C. Huang, and C.-C. Chiang, "Metal-coated fiber Bragg grating for dynamic temperature sensor," *Optik-International Journal for Light and Electron Optics,* vol. 127, pp. 10740-10745, 2016.

[16] S. Baruah, "Dutta J (2009a) Hydrothermal growth of ZnO nanostructures," *Sci Technol Adv Mater,* vol. 10, pp. 013001-013019.

[17] T. Bora, H. Fallah, M. Chaudhari, T. Apiwattanadej, S. W. Harun, W. S. Mohammed, *et al.*, "Controlled side coupling of light to cladding mode of ZnO nanorod coated optical fibers and its implications for chemical vapor sensing," *Sensors and Actuators B: Chemical,* vol. 202, pp. 543-550, 2014.

[18] A. D. Kersey, M. A. Davis, H. J. Patrick, M. LeBlanc, K. Koo, C. Askins, *et al.*, "Fiber grating sensors," *Journal of lightwave technology,* vol. 15, pp. 1442-1463, 1997.

[19] Q. Yao, H. Meng, W. Wang, H. Xue, R. Xiong, B. Huang, *et al.*, "Simultaneous measurement of refractive index and temperature based on a core-offset Mach–Zehnder interferometer combined with a fiber Bragg grating," *Sensors and Actuators A: Physical,* vol. 209, pp. 73-77, 2014.

[20] K. H. Lee, M. Sim, M. Ryu, J. H. Shin, J. E. Jang, J. I. Sohn, *et al.*, "Zinc oxide nanowire-based pressure and temperature sensor," in *Nanotechnology (IEEE-NANO), 2015 IEEE 15th International Conference on*, 2015, pp. 901-904.

[21] J. Huso, J. L. Morrison, H. Che, J. P. Sundararajan, W. J. Yeh, D. McIlroy, *et al.*, "ZnO and MgZnO nanocrystalline flexible films: optical and material properties," *Journal of Nanomaterials,* vol. 2011, p. 30, 2011.